

**ATTACHMENT 3**

**WCAP 13455**

**FRACTURE MECHANICS EVALUATION  
BYRON AND BRAIDWOOD UNITS 1 AND 2  
RESIDUAL HEAT EXCHANGER  
TUBE SIDE INLET AND OUTLET NOZZLES**

**AUGUST 1992**

**(NON-PROPRIETARY)**

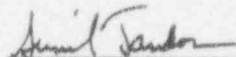
WCAP 13455

FRACTURE MECHANICS EVALUATION  
BYRON AND BRAIDWOOD UNITS 1 AND 2  
RESIDUAL HEAT EXCHANGER  
TUBE SIDE INLET AND OUTLET NOZZLES

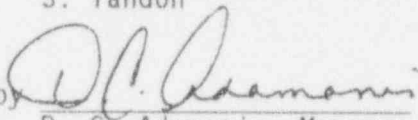
August 1992

W. H. Bamford  
H. Jambusaria  
Y. S. Lee  
J. P. Houstrup

Reviewed by

  
S. Tandon

Approved by



D. C. Adamonis, Manager  
Structural Mechanics Technology

WESTINGHOUSE ELECTRIC CORPORATION  
Nuclear and Advanced Technology Division  
P.O. Box 355  
Pittsburgh, Pennsylvania 15230-355

© 1992 Westinghouse Electric Corp.  
All Rights Reserved

## TABLE OF CONTENTS

### 1.0 INTRODUCTION

- 1.1 Code Acceptance Criteria: Class 1 Components
- 1.2 Acceptance Criteria for Class 2 Components
- 1.3 Geometry

### 2.0 LOADING CONDITIONS, FRACTURE ANALYSIS METHODS, AND MATERIAL PROPERTIES

- 2.1 Transients
- 2.2 Stress Intensity Factor Calculations
- 2.3 Fracture Toughness
- 2.4 Thermal Aging
- 2.5 Allowable Flaw Size Calculation

### 3.0 SUBCRITICAL CRACK GROWTH

- 3.1 Analysis Methodology
- 3.2 Crack Growth Rate Reference Curves
- 3.3 Residual Stresses
- 3.4 Stress Corrosion Cracking Susceptibility

### 4.0 SUMMARY AND RESULTS

- 4.1 Flaw Evaluation Charts Construction
- 4.2 Conservatisms in the Flaw Evaluation

### 5.0 REFERENCES

APPENDIX A: Development of Unified Flaw Acceptance Criteria for Austenitic Piping

APPENDIX B: Welding Procedures and Shop Travellers: Byron and Braidwood Residual Heat Exchangers

## SECTION 1.0 INTRODUCTION

This fracture mechanics evaluation has been carried out to determine the largest size of indications which can be accepted for the residual heat exchanger inlet and outlet nozzles. The results of this evaluation are presented in the form of flaw evaluation charts contained in Section 4. The technical basis for these charts is contained in the remaining sections, and also in Appendix A.

### 1.1 Code Acceptance Criteria: Class 1 Components

The evaluation procedures and acceptance criteria for indications in Class 1 austenitic stainless piping are contained in paragraph IWB 3640 of the ASME Boiler and Pressure Vessel Code, Section XI.[1] The evaluation procedure is applicable to all the materials within a specified distance from the weld centerline,  $\sqrt{rt}$ , where  $r$  = the pipe nominal outside radius and  $t$  is the nominal wall thickness. For example, at the RHX nozzle, this distance is calculated to be 1.62 inches, which encompasses regions of the heat exchanger, as well as part of the RHR line. All the materials in this region are SA 240 Type 304 stainless steel, but these acceptance criteria are applicable for all grades of Types 304 and 316 stainless steels.

The evaluation process begins with a flaw growth analysis, with the requirement to consider growth due to both fatigue and stress corrosion cracking. For pressurized water reactors only fatigue crack growth needs be considered, as discussed in Section 3. The methodology for the fatigue crack growth analysis is described in detail in Section 3.

The calculated maximum flaw dimensions at the end of the evaluation period are then compared with the maximum allowable flaw dimensions for both normal operating conditions and emergency and faulted conditions, to determine acceptability for continued service. Provisions are made for considering flaws projected both circumferentially and axially.



The allowable flaw sizes have been defined in the tables of IWB 3640 based on maintaining specified safety margins on the loads at failure. These margins are 2.77 for normal and upset conditions and 1.39 for emergency and faulted conditions. The calculated failure loads are different for the base metal and the flux welds as they have different fracture toughness values, as discussed in Section 2. (Non-flux welds, such as gas tungsten arc welds, have the same properties as the base metal.) The failure loads, and consequently the allowable flaw sizes are larger for the base metal than for the welds. Allowable flaw sizes for welds are contained in separate tables in IWB 3640.

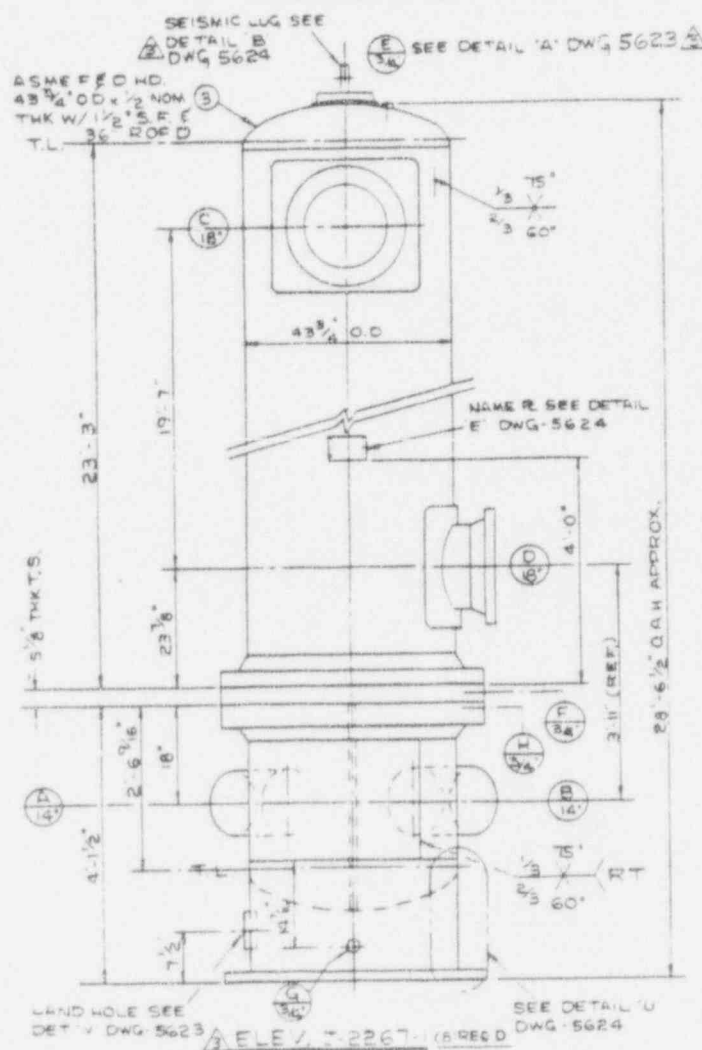
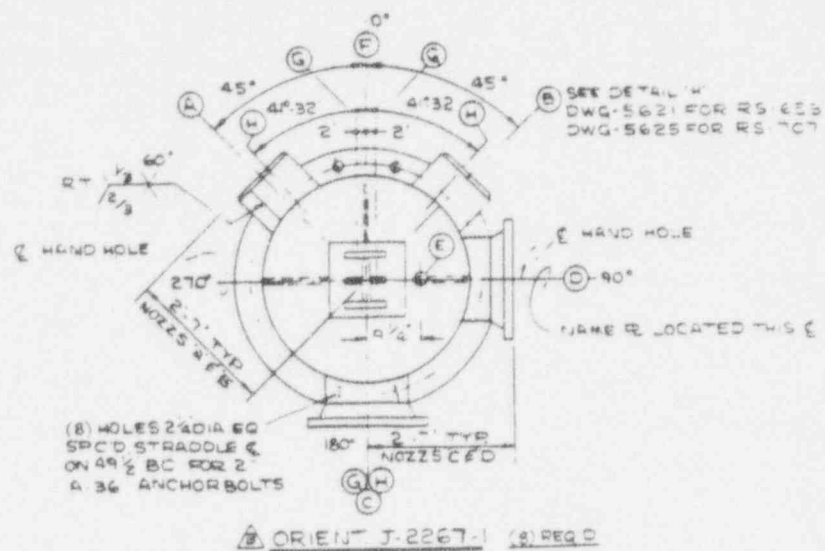
## 1.2 Acceptance Criteria for Class 2 Components

Section XI in its present form contains no acceptance criteria specific to Class 2 components. Instead, the user is referred to the criteria for Class 1 components, which have been described above. Work has been underway for some time in the Section XI committee to develop evaluation criteria for Class 2 and Class 3 components. This work has been used to develop a flaw evaluation chart specific to the Byron and Braidwood Residual Heat Exchangers. The detailed technical basis is contained in Appendix A of this report. This approach is consistent with the approach used for Class 1 components, and in fact allows one to reproduce the acceptance criteria for Class 1 systems. The approach utilizes the original design criteria for the component and maintains this design margin in the presence of a flaw. The corrections for flux welds are exactly the same as those for Class 1 components.

## 1.3 Geometry

The geometry of the residual heat exchanger is shown in Figure 1-1, the details of the inlet and outlet nozzles of the tube side is shown in Figure 1-2. The tube side of the residual heater exchanger is designed to Class 2 criteria, while the shell side is designed as Class 3. The notation used for surface and embedded flaws in this work is illustrated in Figure 1-3.

The fracture and fatigue crack growth evaluations carried out to develop the handbook charts have employed the recommended procedures and material properties for stainless steel prescribed in paragraph IWB 3640 and Appendix C of Section XI.



WPFO863/111191:10

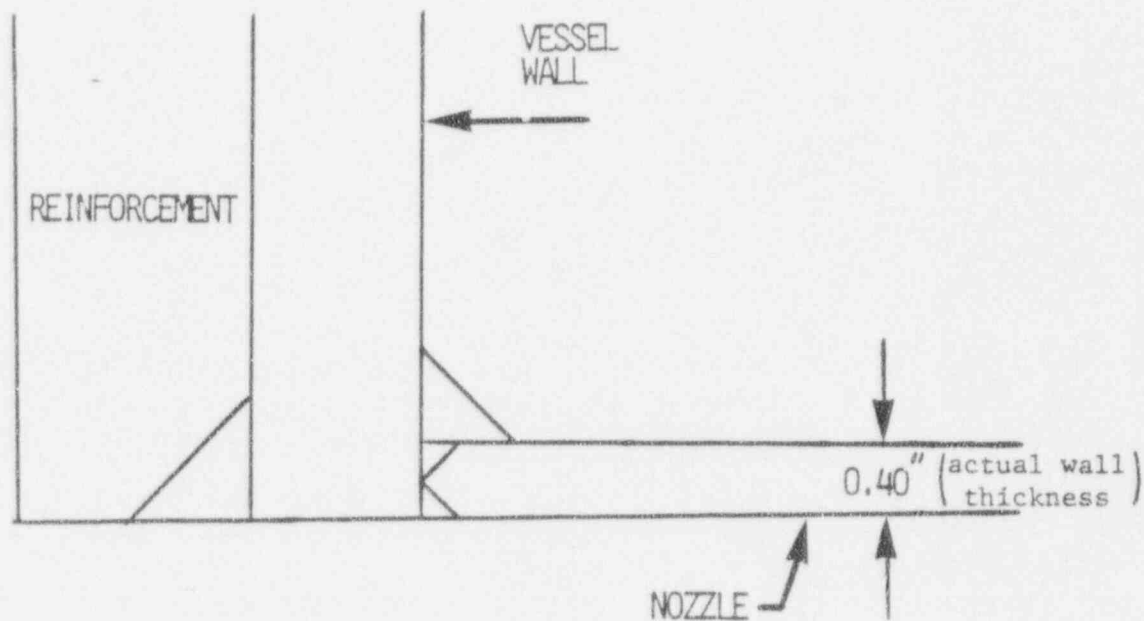
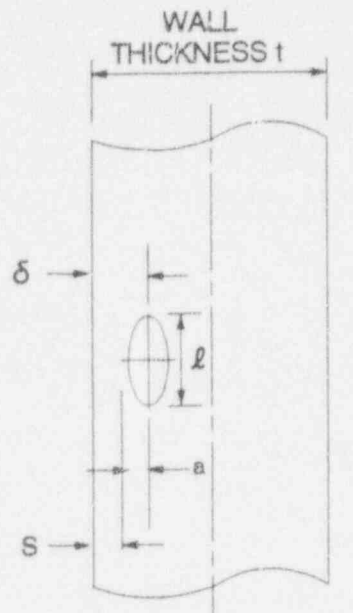
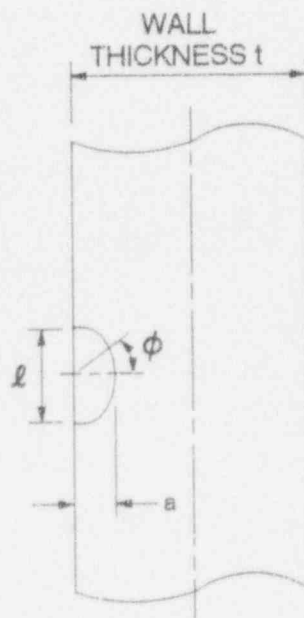


Figure 1-2. Geometry of the Tube Side Nozzles  
(Inlet and Outlet Nozzles are Identical)



TYPICAL EMBEDDED FLAW INDICATION



TYPICAL SURFACE FLAW INDICATION

Figure 1-3. Typical Notation for Surface and Embedded Flaw Indications

## SECTION 2.0

### LOAD CONDITIONS, FRACTURE ANALYSIS METHODS AND MATERIAL PROPERTIES

The loading conditions used in the analyses described herein were taken directly from the equipment specification. The latest fracture analysis technology has been employed in conducting this analysis. The material properties have been taken from the latest version of the Reference 1 ASME Code.

#### 2.1 Transients and Load Conditions

The design transients for the residual heat exchanger are very minimal, because this component operates only during plant shutdown conditions. Therefore, the only transient conditions which it experiences are the startup and shutdown of the system. This coincides with the shutdown and startup of the plant, respectively. The appropriate limiting load conditions for the location of interest are discussed next.

The loading conditions which were evaluated include thermal expansion (normal and upset), pressure, deadweight and seismic (OBE and SSE) loadings. The RHR piping forces and moments for each condition were obtained from the ASME Code Section III calculations performed by Sargent and Lundy and Westinghouse for Byron and Braidwood Units 1 and 2 in References 2 through 5. These loads [6] were found to be bounded by the equipment specification design loadings for the heat exchanger nozzles (G-679150 Rev. 1). Consequently, the evaluation performed using the design loadings is applicable to Byron and Braidwood Units 1 and 2. Residual stresses were not used in this portion of the evaluation in compliance with the Code guidelines. A further discussion of residual stresses is contained in Section 3.2. The stress intensity values were calculated using the following equations:

$$SI = P_m + P_b$$

$$SI = \frac{F_r}{A} + \frac{1}{Z} [M_x^2 + M_y^2 + M_z^2]^{0.5}$$

where

$F_x$  = axial force component (membrane)

$M_x, M_y, M_z$  = moment components (bending)

$A$  = cross-section area

$Z$  = section modulus

The section properties  $A$  and  $Z$  at the weld location were determined based on the minimum pipe dimensions. This is conservative since the measured wall thickness at the weld is generally larger.

The following load combinations were used.

A. Normal/Upset - Primary Stress

Pressure + Deadweight + OBE

B. Emergency/Faulted - Primary Stress

Pressure + Deadweight + SSE

C. Normal/Upset - Total Stress

Pressure + Deadweight + OBE + Normal Thermal

D. Emergency/Faulted - Total Stress

Pressure + Deadweight + SSE + Normal Thermal

## 2.2 Stress Intensity Factor Calculations

One of the key elements of the fatigue crack growth calculations is the determination of the driving force inherent to the flaw, or stress intensity factor ( $K_I$ ). This was done using expressions from available literature. In all cases the stress intensity factor calculations utilized a representation of the actual stress profile rather than a linearization. This was necessary

to provide the most accurate determination possible. The stress profile was represented by a cubic polynomial:

$$\sigma(x) = A_0 + A_1 \frac{x}{t} + A_2 \left( \frac{x}{t} \right)^2 + A_3 \left( \frac{x}{t} \right)^3 \quad (2-1)$$

where  $x$  is the coordinate distance into the wall  
 $t$  = wall thickness  
 $\sigma$  = stress perpendicular to the plane of the crack  
 $A_i$  = coefficients of the cubic fit

For the surface flaw with length six times its depth, the stress intensity factor expression of [McGowan and Raymond [ ]]<sup>a,c,e</sup> was used. The stress intensity factor  $K_I(\phi)$  can be calculated anywhere along the crack front. The point of maximum crack depth is represented by  $\phi = 0$ . The following expression is used for calculating  $K_I(\phi)$ , where  $d$  is the angular location around the crack.

$$K_I(\phi) = \left[ \frac{\pi a}{Q} \right]^{0.5} (\cos^2 \phi + \frac{a^2}{C^2} \sin^2 \phi)^{1/4} (A_0 H_0 + \frac{2}{\pi} \frac{a}{t} A_1 H_1 + \frac{1}{2} \frac{a^2}{t^2} A_2 H_2 + \frac{4}{3\pi} \frac{a^3}{t^3} A_3 H_3) \quad (2-2)$$

The magnification factors  $H_0(\phi)$ ,  $H_1(\phi)$ ,  $H_2(\phi)$  and  $H_3(\phi)$  are obtained by the procedure outlined in reference [8].

The stress intensity factor calculation for a semi-circular surface flaw, (aspect ratio 2:1) was carried out using the expressions developed by [ ]<sup>a,c,e</sup>. Their expression utilizes the same cubic representation of the stress profile and gives precisely the same result as the expression of [ ]<sup>a,c,e</sup> for the 6:1 aspect ratio flaw, and the form of the equation is similar to that of [ ]<sup>a,c,e</sup> above.

The stress intensity factor expression used for a continuous surface flaw was that developed by [ ]<sup>a,c,p</sup>. Again the stress profile is represented as a cubic polynomial, as shown above, and these coefficients as well as the magnification factors are combined in the expression for  $K_I$

$$K_I = \sqrt{\pi a} \left[ \begin{array}{c} F_1 \\ F_2 \\ F_3 \\ F_4 \end{array} \right]^{a,c,p} \quad (2-3)$$

where  $F_1, F_2, F_3, F_4$  are magnification factors, available in [9].

### 2.3 Fracture Toughness

The residual heat exchanger is constructed of SA 240 stainless steel, type 304. The weld at the nozzle was made by the shielded metal arc process as verified by the shop traveller and the weld procedure referenced therein.

The fracture toughness of the base metal has been found to be relatively very high, even at operating temperatures [10], where the  $J_{Ic}$  values have been found to be well over 2000 in-lb/in<sup>2</sup>. Fracture toughness values for weld materials have been found to display much more scatter, with the lowest reported values significantly lower than the base metal toughness. Although the  $J_{Ic}$  values reported have been lower, the slope of the J-R-curve is still large for these  $J_{Ic}$  cases. Representative values for  $J_{Ic}$  were obtained from the results of Landes, et. al. [11], and used in the development of the fracture evaluation methods.

[ ]<sup>a,c,p</sup>

This value of toughness was used in the original development of the flaw acceptance criteria, and has been shown to be extremely conservative relative to test results for larger specimens obtained since that time. This subject is further discussed in Section 4.2.



## 2.4 THERMAL AGING

Thermal aging at operating temperatures of reactor primary piping can reduce the fracture toughness of cast stainless steels and, to a lesser degree, stainless steel weldments. Because of the lower operating temperature (400°F) of the residual heat exchanger, and the fact that the materials are type 304 stainless (not cast), thermal aging in this component will be negligible.

## 2.5 Allowable Flaw Size Determination

The critical flaw size is not directly calculated as part of the flaw evaluation process for stainless steels. Instead, the failure mode and critical flaw size are incorporated directly into the flaw evaluation technical basis, and therefore into the tables of "Allowable End-of-Evaluation Period Flaw Depth to Thickness Ratio," which are contained in paragraph IWB 3640. The same is true for the revised acceptance criteria for Class 2 components.

Rapid, nonductile failure is possible for ferritic materials at low temperatures, but is not applicable to stainless steels. In stainless steel materials, the higher ductility leads to two possible modes of failure, plastic collapse or unstable ductile tearing. The second mechanism can occur when the applied J integral exceeds the  $J_{Ic}$  fracture toughness and some stable tearing occurs prior to failure. If this mode of failure is dominant, the load carrying capacity is less than that predicted by the plastic collapse mechanism.

The allowable flaw sizes of paragraph IWB 3640 for the high toughness base materials were determined based on the assumption that plastic collapse would be achieved and would be the dominant mode of failure. [

] a.c.e

## SECTION 3.0

### FATIGUE CRACK GROWTH

In applying Code acceptance criteria as introduced in Section 1, the final flaw size  $a_f$  is defined as the flaw size to which the detected flaw is calculated to grow at the end of a specified period, or until the next inspection time. This section will examine each of the calculations, and provide the methodology used as well as the assumptions.

#### 3.1 Analysis Methodology

The methods used in the crack growth analysis reported here are the same as those suggested by Section XI of the ASME Code. The analysis procedure involves postulating an initial flaw at specific regions and predicting the growth of that flaw due to an imposed series of loading transients. The input required for a fatigue crack growth analysis is basically the information necessary to calculate the parameter  $\Delta K_I$  which depends on crack and structure geometry and the range of applied stresses in the area where the crack exists. Once  $\Delta K_I$  is calculated, the growth due to that particular stress cycle can be calculated by equations given in Section 2.2 and figure 3-1. This increment of growth is then added to the original crack size, and the analysis proceeds to the next transient. The procedure is continued in this manner until all the transients known to occur in the period of evaluation have been analyzed.

The only transients considered in the analysis were the startup and shutdown of the RHR system. These transients are spread equally over the design lifetime of the vessel.

Crack growth calculations were carried out for a range of flaw depths of three basic types. The first two types were surface flaws, one with length equal to six times the depth and another with length equal to twice the depth. The third type was a continuous surface flaw which represents a worst case condition for surface flaws.

### 3.2 Crack Growth Rate Reference Curves

The reference crack growth law used for the stainless steel was taken from that developed by the Metal Properties Council - Pressure Vessel Research Committee Task Force in Crack Propagation Technology. The reference curve has the equation:

$$\frac{da}{dN} = CFS \Delta K^n \quad (3-7)$$

where  $\frac{da}{dN}$  = crack growth rate, inches per cycle

- C = Material coefficient ( $C = 2.0 \times 10^{-19}$ )
- F = Frequency coefficient for loadings ( $F = 2.0$ )
- S = R ratio correction coefficient ( $S = 1.0 = 0.502 R^2$ )<sup>-4.0</sup>
- n = Material property slope (=3.0321)
- $\Delta K$  = Stress intensity factor range, psi  $\sqrt{\text{in}}$

This equation appears in Section XI, Appendix C (1989 Addendum) for air environments and its basis is provided in reference [12], and shown in figure 3-1. For water environments, an environmental factor of 2 was used, based on the crack growth tests in PWR environments reported by Bamford [13].

### 3.3 Residual Stresses

Since the residual heat exchanger vessel-to-piping welds have not been stress-relieved, residual stresses are likely present. For fatigue crack growth analyses, these stresses are included directly.

In general, the distribution of residual stresses is strongly dependent on the degree of constraint of the structure. The stiffer the structure, the higher the residual stresses. [

] 6.5.8

[

] s.c.e

[

] s.c.e

### 3.4 Stress Corrosion Cracking Susceptibility

In evaluating flaws, all mechanisms of subcritical crack growth must be evaluated to ensure that proper safety margins are maintained during service. Stress corrosion cracking has been observed to occur in stainless steel in operating BWR piping systems. The discussion presented here is the technical basis for not considering this mechanism in the present analysis. The residual heat exchanger tube side nozzles are exposed to only primary coolant water.

For all Westinghouse plants, there is no history of cracking failure in the reactor coolant system loop piping. For stress corrosion cracking (SCC) to occur in piping, the following three conditions must exist simultaneously: high tensile stresses, a susceptible material, and a corrosive environment. Since some residual stresses and some degree of material susceptibility exist in any stainless steel piping, the potential for stress corrosion is minimized by proper selection of a material immune to SCC as well as preventing the occurrence of a corrosive environment. The material specifications have taken into consideration compatibility with the system's operating environment (both internal and external) as well as other materials in the system, applicable ASME Code rules, fracture toughness, welding, fabrication, and processing.

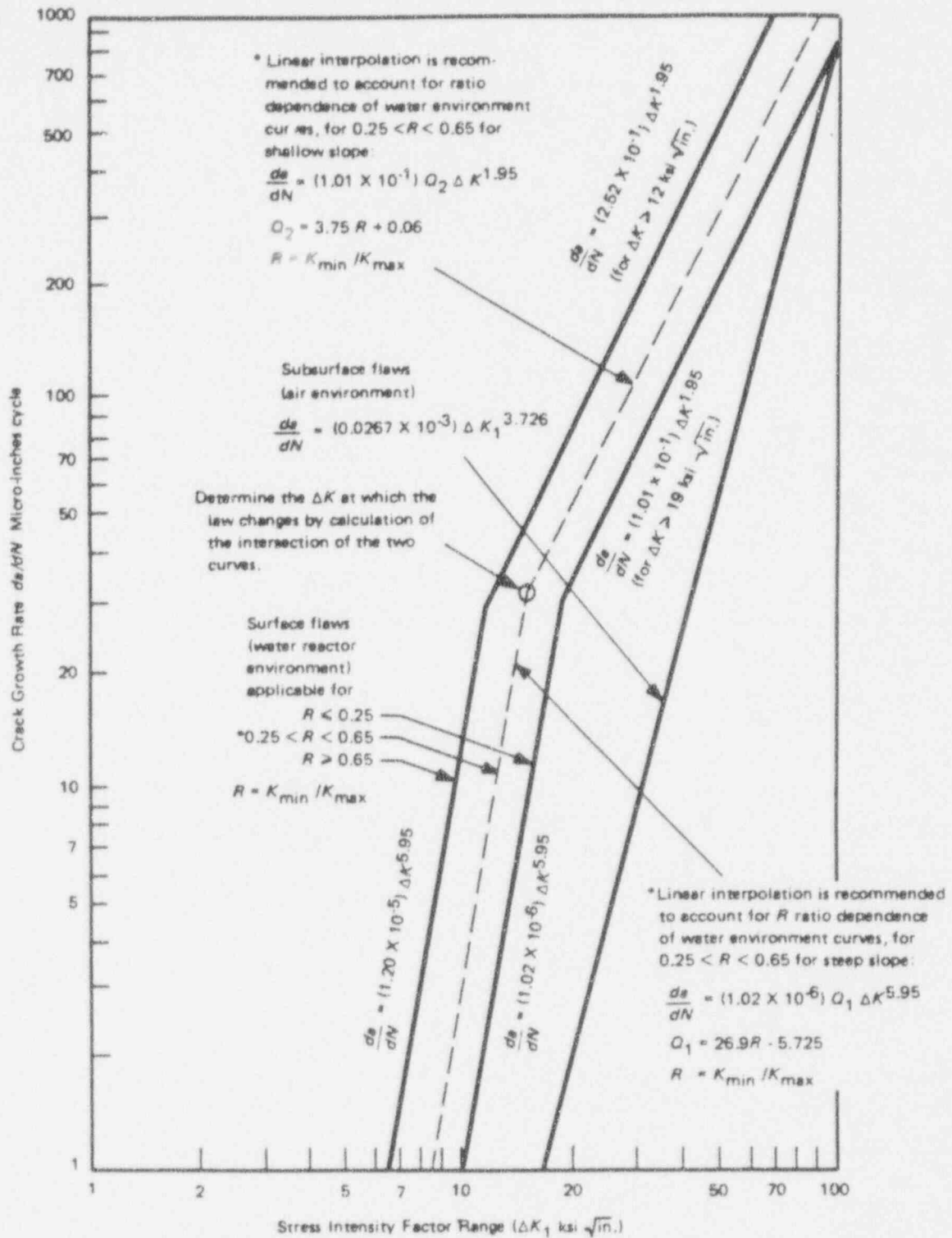


Figure 3-1. Reference Crack Growth Rate Curves for Stainless Steel in Air Environments [12].

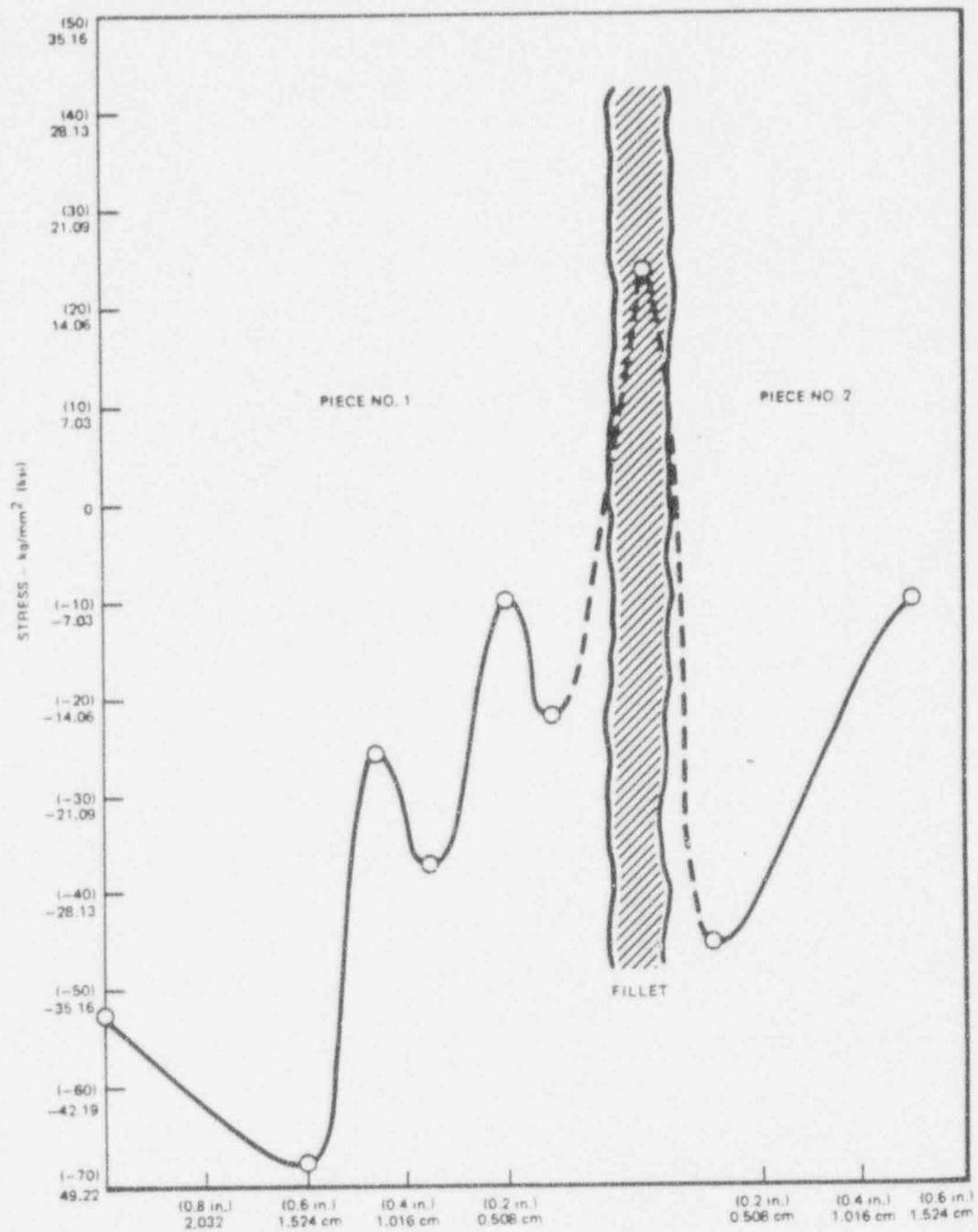


Figure 3-2. Maximum Principal Surface Residual Stress for a 10 inch Schedule 160 Pipe [14]

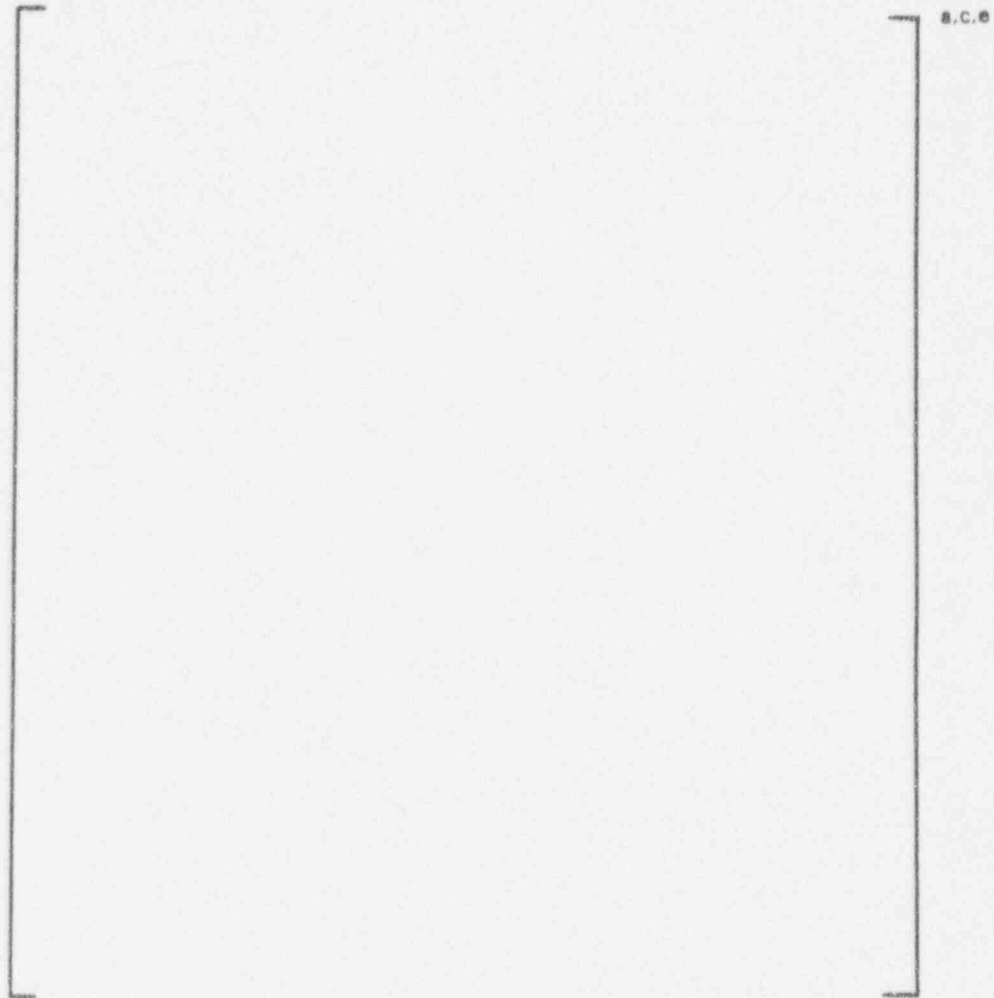


Figure 3-3. Through Wall Distribution of Residual Stress in a 10 Inch, Schedule 160 Pipe, in a Cross Section Adjacent to the Weld Center Line [15]

## SECTION 4.0

### SUMMARY AND RESULTS

#### 4.1 Flaw Evaluation Charts Construction

The acceptance criteria for surface flaws have been described in Section 1 for both Class 1 and Class 2 components. For flaw evaluation in stainless steels, only the fatigue crack growth results must be calculated. The allowable flaw depths were determined directly from the tables in IWB 3640 and from tables developed specifically for Class 2 components, as detailed in Appendix A.

The first set of data required for surface flaw chart construction is the final flaw size  $a_f$ . As defined in IWB-3611 of ASME Code Section XI,  $a_f$  is the flaw depth resulting from growth during a specific time period which can be the next scheduled inspection of the component or until the end of design lifetime. Therefore, the final depth,  $a_f$ , after a specific service period of time must be used as the basis for evaluation.

The final flaw size,  $a_f$ , can be calculated by fatigue crack growth analysis, which has been performed covering a range of postulated flaw sizes, and flaw shapes. The crack growth calculational methods have been discussed in Section 3. The results of the crack growth calculation showed that growth for a complete range of crack sizes was inconsequential for the entire service life of 40 years. This was expected, since the region experiences so few cycles.

The allowable flaw size for Class 1 stainless steel piping and components is obtained directly from tables in paragraph IWB 3640, so the evaluation process is straightforward. The allowable flaw size for Class 2 piping and components was obtained directly through use of Appendix A.

The allowable flaw size is calculated based on the most limiting transient for all normal operating conditions. Similarly, the allowable flaw size for emergency and faulted conditions is also determined. The theory and methodology for the calculation of the allowable flaw sizes have been provided in Section 2 and Reference 16 for Class 1 components, and in Appendix A for Class 2 components. Allowable flaw sizes were calculated for a range of flaw shapes.



Two dimensionless parameters which fully address the characteristics of a surface flaw, have been used for the evaluation chart construction:

- o Flaw Length divided by the circumference,  $\ell/c$
- o Flaw Depth parameter  $a/t$

where,

- t = wall thickness, in.
- a = flaw depth, in.
- $\ell$  = flaw length, in.
- c = pipe circumference, in.

The flaw evaluation chart for the residual heat exchanger inlet and outlet nozzles is shown in Figure 4-1. The chart has the following characteristics:

[

] a.c.#

A detailed example on the use of the charts for a surface flaw is presented below:

#### Surface Flaw Example

Now suppose an indication is to be evaluated using the charts. For the circumferential orientation:

$$\begin{array}{ll} a = 0.10" & l = 6.1" \\ t = 0.40" & c = 44.0" \end{array}$$

The flaw characterization parameters then become:

$$\begin{array}{l} a/t = 0.250 \\ l/c = 0.139 \end{array}$$

Plotting these parameters on the surface flaw evaluation chart of Figure 4-1, it is quickly seen that the indication is acceptable, for both the class 1 and class 2 curves.

#### Embedded Flaw Example

The flaw evaluation charts are equally useful for embedded flaws. Suppose an embedded indication were discovered with the following dimensions:

$$\begin{array}{lll} 2a = 0.2" & l = 7.0" & S = 0.1" \\ t = 0.4" & c = 44.0" & \end{array}$$

The indication would be characterized as an embedded flaw, because the S dimension exceeds 0.4a. The flaw characterization parameters then become:

$$\begin{array}{l} 2a/t = .5 \\ l/c = 0.160 \end{array}$$

Plotting these parameters on the flaw evaluation chart in Figure 4-1 shows that the indication is acceptable for both the Class 1 and Class 2 acceptance

criteria. Note that for embedded flaws, the total depth "2a" of the flaw is plotted on the chart.

#### 4.2 Conservatisms in the Flaw Evaluation

The stress and fracture analysis results presented herein have been structured to be conservative at each step to ensure conservatism in the final result.

The stresses applied to the heat exchanger nozzles were taken from the vessel equipment specification loads, which represent bounding loads for the structure. The actual loads for the Byron and Braidwood Units 1 and 2 heat exchangers [6] are approximately 60 percent of the design loads.

[

] a.c.e

Figure 4-1 Flaw Evaluation Chart for Byron and Braidwood Units 1 and 2  
Residual Heat Exchanger Tube Side Nozzles

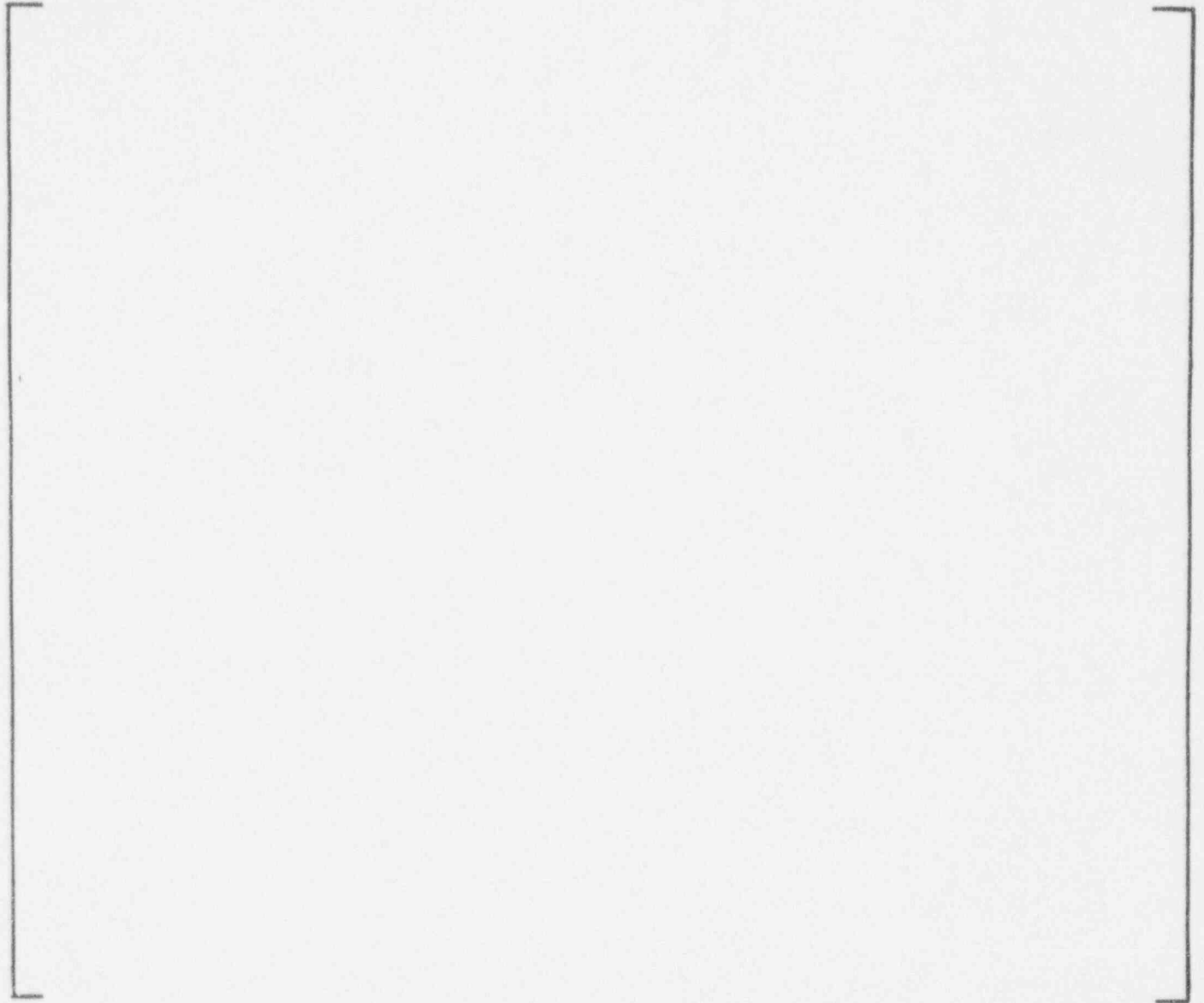


Figure 4-2 Comparison of Fracture Toughness Results for Different Specimen Sizes, Submerged Arc Weldments

## SECTION 5.0

### REFERENCES

1. ASME Code Section XI, "Rules for Inservice Inspection of Nuclear Power Plant Components," 1983 edition (used for updated code allowable limits); 1983 edition, Winter 1985 Addendum (used for flaw evaluation of austenitic stainless steel piping); 1989 edition (used for reference crack growth curve, stainless steel).
2. Jambusaria, H., "Residual Heat Exchangers: Braidwood Unit 2," Westinghouse Report No. 031804 Rev. 0, Jan. 24, 1986.
3. Jambusaria, H., "Residual Heat Exchangers: Byron Unit 1," Westinghouse Report No. 031805 Rev. 0, 2/27/92.
4. Jambusaria, H., "Residual Heat Exchangers: Byron Unit 2," Westinghouse Report No. 031806 Rev. 0, 2/27/92.
5. Jambusaria, H., "Residual Heat Exchangers: Braidwood Unit 1," Westinghouse Report No. 031803 Rev. 0, 2/27/92.
6. Letter #BPM #1577 from D. J. Skoza of Commonwealth Edison Company to Janet Bunecicky of Westinghouse Electric Corporation, Subject: RHR Heat Exchanger Nozzle Loads, dated 2/12/92.
7. McGowan, J. J. and Raymund, M., "Stress Intensity Factor Solution for Internal Longitudinal Semi-elliptic Surface Flaw in a Cylinder Under Arbitrary Loading", ASTM STP 677, 1979, pp. 365-380.
8. Newman, J. C. Jr. and Raju, I. S., "Stress Intensity Factors for Internal Surface Cracks in Cylindrical Pressure Vessels", ASME Trans., Journal of Pressure Vessel Technology, Vol. 102, 1980, pp. 342-346.
9. Buchalet, C. B. and Bamford, W. H., "Stress Intensity Factor Solutions for Continuous Surface Flaws in Reactor Pressure Vessels", in Mechanics of Crack Growth, ASTM, STP 59C, 1976, pp. 385-402.

10. Bamford, W. H. and Bush, A. J., "Fracture of Stainless Steel," in Elastic Plastic Fracture, ASTM STP 668, 1979.
11. Landes, J. D., and Norris, D. M., "Fracture Toughness of Stainless Steel Piping Weldments," presented at ASME Pressure Vessel Conference, 1984.
12. James, L. A., and Jones, D. P., "Fatigue Crack growth Correlations for Austenitic Stainless Steel in Air," in Predictive Capabilities in Environmentally Assisted Cracking, ASME publication PVP-99, Dec. 1985.
13. Bamford, W. H., "Fatigue Crack Growth of Stainless Steel Piping in a Pressurized Water Reactor Environment," Trans ASME, Journal of Pressure Vessel technology, Feb. 1979.
14. "Studies on AISI Types 304, 304L, and 347 Stainless Steels for BWR Application, April-June 1975," General Electric Report NEDO-20985-1, September 1975.
15. Rybicki, E. F., McGuire, P. A., Merrick, E., and West, J., "The Effect of Pipe Wall Thickness on Residual Stresses Due to Girth Welds," Trans ASME, Journal of Pressure Vessel Technology, Vol 104, August 1982.
16. "Evaluation of Flaws in Austenitic Steel Piping," Trans ASME, Journal of Pressure Vessel Technology, Vol. 108, Aug. 1986, pp. 352-366.
17. Wilkowski, G. et. al., "Analysis of Experiments on Stainless Steel Flux Welds," Battelle Columbus labs report for USNRC, number NUREG/CR 4878, April 1987.

APPENDIX A  
DEVELOPMENT OF UNIFIED FLAW ACCEPTANCE  
CRITERIA FOR AUSTENITIC PIPING

A.1.0 INTRODUCTION

There are currently rules in the ASME B&PV Code, Section XI, (Ref.(A3)), for the evaluation of flaws in austenitic piping when the discovered indications exceed the allowable acceptance standards. These rules are complex, use relatively arbitrary "safety factors", require the knowledge of a "flow stress" that is very difficult to determine, and have arbitrary limits on the maximum flaw depths allowed, with the result that the compounded conservatisms have produced very conservative results.

The approach taken in developing these rules is that austenitic piping is very ductile and a failure of a pipe, whether flawed or not, will be by plastic collapse of the pipe cross section and has been verified by numerous experiments. A solution for the collapse load of a flawed pipe was developed in terms of the applied primary loads and the flawed pipe geometry using limit load theory with the yield stress replaced by a flow stress. This collapse stress is divided by a fixed safety factor (2.77 for Level A and B loadings and 1.39 for Level C and D loadings) to establish allowable stresses in the flawed pipe and these were back calculated to establish the allowable flaw size. It should be noted that the collapse equations were developed for a thin walled tube ( $R \gg t$ ), for this is the only practical solution, and again is conservative for real pipes which have thicker cross sections.

These solutions of Ref. (A3) have several limitations:

- a) They are available for Class 1 piping only.
- b) The allowable design stresses of Ref. (A1) have different values for each of the loading categories (Levels A, B, C, and D) that are not always consistent with the safety factors used.



- c) The accumulated conservatisms are such that, for many cases, a new unflawed pipe will fail the criteria of Ref. (A3).
- d) There is no limit on axial membrane stress. Although the predominant failure mode in piping is by bending, there are cases such as a flaw in an end cap weld where the membrane stress governs.

[ ]<sup>a,c,e</sup>

## A.2.0 CRITERIA

The criteria of the ASME B&PV Code, Section III, "Nuclear Power Plant Components", (Ref. (A1)) for the design of new components is based upon the premise that the materials used will be ductile and the failure mode will be by plastic collapse. The resulting minimum safety margin is the ratio of the collapse load of the structure to the maximum permitted loads in the structure. The collapse load of the structure is conservatively defined in Section III using limit load theory with the collapse stress equal to the yield strength of the material. These criteria are discussed in "Criteria of Section III of the ASME Boiler and Pressure Vessel Code for Nuclear Vessels", ASME, 1964 (Ref. (A2)). Figure A2.1 is a reproduction of Fig. 2 of Ref. (A2) that demonstrates the safety margins for a beam of rectangular cross section for both longitudinal membrane and membrane plus bending stresses.

[ ]<sup>a,c,d</sup>

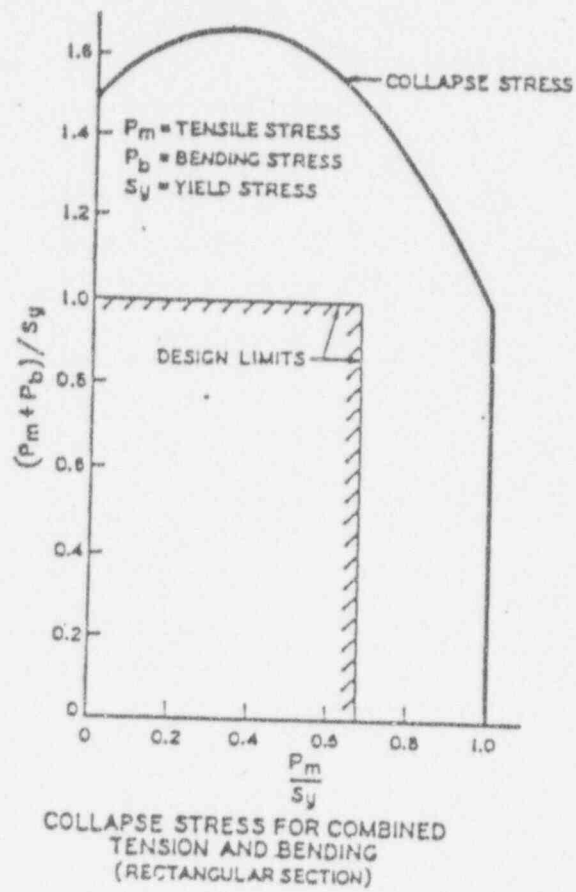


Figure A2.1 Reproduction of Figure 2 of Reference A2

[ ] 8, C, 8

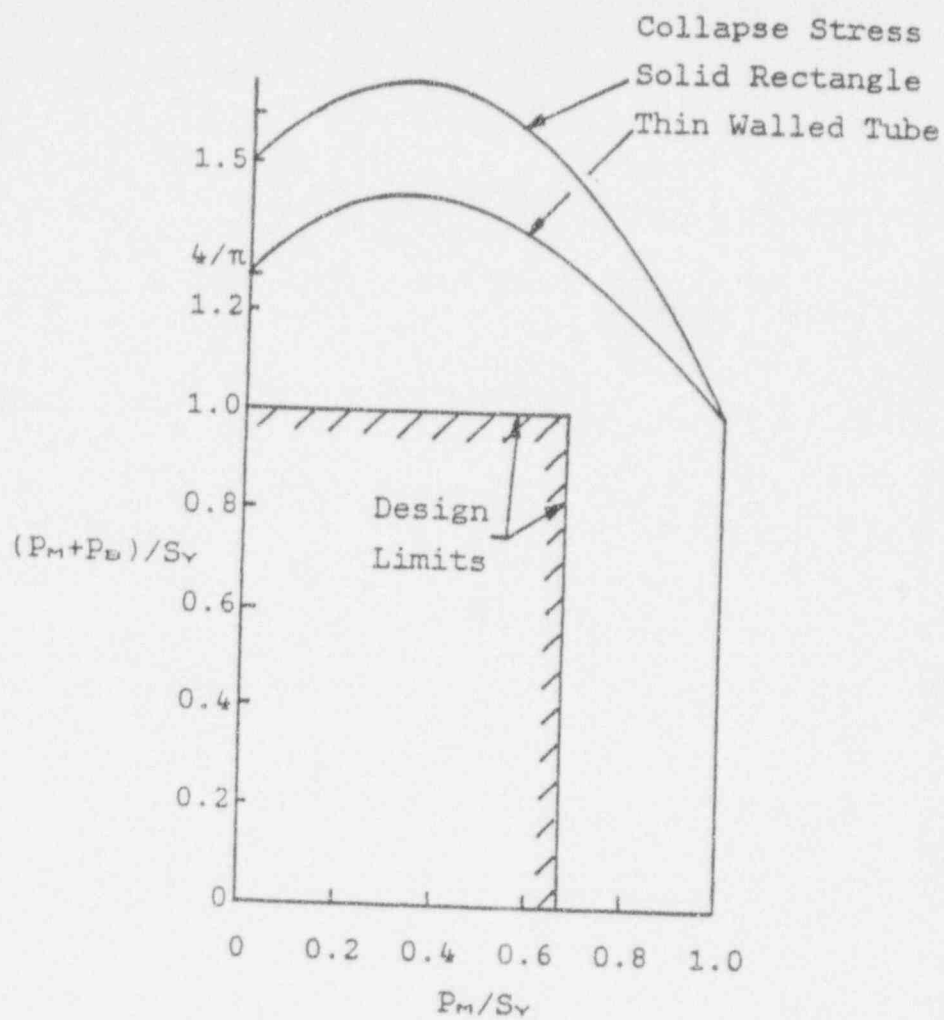


Figure A2.2 Collapse curve for a thin walled tube  
for comparison with Fig. A2.1

[ ]a,c,e

### A.3.0 FLAW NOMENCLATURE FOR A CIRCUMFERENTIAL FLAW

The nomenclature used in evaluating a pipe with a circumferential flaw is illustrated in Figure A3.1 and defined specifically as:

- $a$  = the maximum measured flaw depth projected to the end of the evaluation period.
- $\Theta$  = the maximum measured half flaw length in radians projected to the end of the evaluation period.
- $\beta$  = angle in radians to the neutral axis.
- $t$  = pipe wall thickness.
- $R$  = mean radius of pipe.
- $R_i$  = inside radius of pipe.
- $R_o$  = outside radius of pipe.
- $\sigma_f$  = flow stress at plastic collapse.

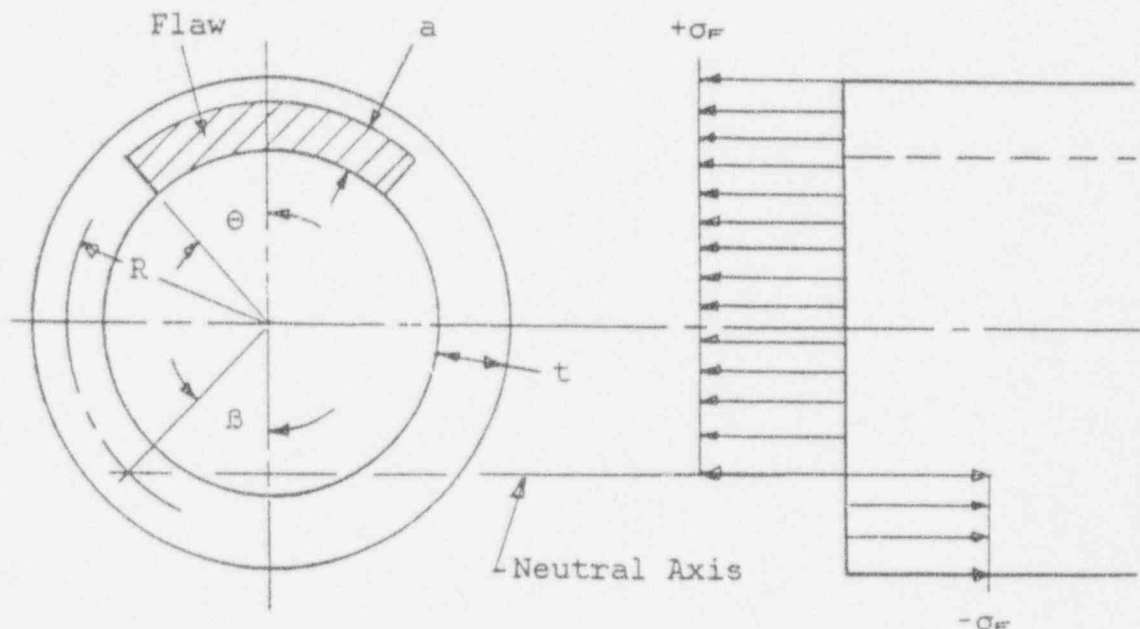


Figure A3.1 cross section of flawed pipe.

#### A.4.0 FLAW EVALUATION DEVELOPMENT

##### A.4.1 Limit On Membrane Plus Bending Stress

[ ]<sup>8,C,8</sup>

[ ]<sup>8,C,8</sup>

[ ] 8.5.8

[ ]<sup>R.C.B</sup>

[ ]<sup>R.C.B</sup>

FLAW DEPTH RATIO A/T	FLAW LENGTH $\Theta/\pi$									
	0.1	0.2	0.3	0.4	0.5	0.6	0.7	0.8	0.9	1.0
0.1	.984	.970	.958	.950	.947	.947	.947	.947	.947	.947
0.2	.969	.939	.915	.897	.888	.886	.886	.886	.886	.886
0.3	.953	.907	.869	.840	.822	.818	.818	.818	.818	.818
0.4	.936	.875	.821	.778	.751	.740	.739	.739	.739	.739
0.5	.920	.841	.770	.713	.674	.653	.650	.650	.650	.650
0.6	.903	.806	.718	.644	.591	.559	.547	.547	.547	.547
0.7	.886	.770	.663	.572	.503	.457	.435	.431	.431	.431
0.8	.869	.734	.606	.496	.409	.349	.314	.301	.300	.300
0.9	.851	.696	.547	.416	.310	.233	.185	.161	.155	.155

Table A4.2 Calculated values of the flaw reduction factors in equations (7a) and (8a), primary membrane plus bending stresses in a pipe with a circumferential flaw.

#### A.4.2 Limit on Membrane Stress

[ ]<sup>R.C.B</sup>

[ ]<sup>R.C.B</sup>



FLAW DEPTH RATIO A/T	FLAW LENGTH $\Theta/\pi$									
	0.1	0.2	0.3	0.4	0.5	0.6	0.7	0.8	0.9	1.0
0.1	0.99	0.98	0.97	0.96	0.95	0.94	0.93	0.92	0.91	0.90
0.2	0.98	0.96	0.94	0.92	0.90	0.88	0.86	0.84	0.82	0.80
0.3	0.97	0.94	0.91	0.88	0.85	0.82	0.79	0.76	0.73	0.70
0.4	0.96	0.92	0.88	0.84	0.80	0.76	0.72	0.68	0.64	0.60
0.5	0.95	0.90	0.85	0.80	0.75	0.70	0.65	0.60	0.55	0.50
0.6	0.94	0.88	0.82	0.76	0.70	0.64	0.58	0.52	0.46	0.40
0.7	0.93	0.86	0.79	0.72	0.65	0.58	0.51	0.44	0.37	0.30
0.8	0.92	0.84	0.76	0.68	0.60	0.52	0.44	0.36	0.28	0.20
0.9	0.91	0.82	0.73	0.64	0.55	0.46	0.37	0.28	0.19	0.10

Table A4.3 Calculated values of the flaw reduction factors in equation (9), primary membrane stress in piping with a circumferential flaw.

A.5.0 DEVELOPMENT OF ACCEPTANCE CRITERIA FOR THE RESIDUAL HEAT EXCHANGER NOZZLES

[ ]<sup>B.C.R</sup>

The loads from Section 4 and appropriate class 2 allowable stresses are listed below:

Loading Case	$P_m + P_b$ (ksi)	$Z_1$	Allowable Stress $\sigma_A$ (ksi)
Level A	12.3	1.449	$1.5 S_H = 24.3$
Level B	12.3	1.449	$1.8 S_H = 29.2$
Level C	16.8	1.449	$2.25 S_H = 36.45$
Level D	16.8	1.449	$2.0 S_Y = 40.7$

a/t	$\Theta/\pi$			
	Level A	Level B	Level C	Level D
0.1	1.0	1.0	1.0	1.0
0.2	1.0	1.0	1.0	1.0
0.3	1.0	1.0	1.0	1.0
0.4	1.0	1.0	1.0	1.0
0.5	0.365	1.0	0.529	1.0
0.6	0.283	0.462	0.368	0.509
0.7	0.235	0.357	0.295	0.382
0.8	0.201	0.296	0.252	0.316
0.9	0.176	0.257	0.219	0.272

[ ]<sub>R.C.B</sub>

[ ] R.C.A



Figure A5.1 Flaw Evaluation Chart for Residual Heat Exchanger  
Tube Side Inlet and Outlet Nozzles

#### A.6.0 REFERENCES

- (A1) ASME Boiler and Pressure Vessel Code, Section III, "Nuclear Power Plant Components". 1989 Edition with the 1991 Addenda used for specific references.
- (A2) "Criteria of Section III of the ASME Boiler and Pressure Vessel Code for Nuclear Vessels", ASME, 1964.
- (A3) ASME Boiler and Pressure Vessel Code, Section XI, "Rules for Inservice Inspection of Nuclear Power Plant Components". 1989 Edition with the 1991 Addenda used for specific references.
- (A4) J. P. Houstrup; Presentation to the ASME Section XI Task Group on Pipe Flaw Evaluation, in minutes, Nov. 1988.
- (A5) EPRI Report No. NP-4690SR, "Evaluation of Flaws in Austenitic Steel Piping", July, 1986.

## APPENDIX B

### WELDING PROCEDURES AND SHOP TRAVELLERS BYRON AND BRAIDWOOD RESIDUAL HEAT EXCHANGERS



WELDING PROCEDURE SPECIFICATION WPS-9

SHIELDED METAL-ARC WELDING

STAINLESS STEEL TO STAINLESS STEEL

Welding Process:

- A. All welding shall be done by the Shielded Metal-Arc Welding Process (SMAW) in accordance with ASME Section IX.

Base Metals:

- A. Each base metal shall conform to a specification listed in Section IX group P-8.

Filler Metals and Electrodes:

- A. The electrode shall conform to ASME specification number SFA 5.4, group F-5 and Weld Metal Analysis A-8 as indicated in Table A.

Shielding Gas and Backing Rings:

- A. Shielding gas shall not be used.  
B. Gas backing, nonmetallic retainers, or nonfusing metal retainers shall not be used.

Base Metal Thickness:

- A. This procedure covers groove welding of material thicknesses from 3/16" to 1-1/2" and all size fillet welds on any material thickness.

11

Preparation of Base Material:

- A. The edges or surfaces of the parts to be welded may be cut by machining, grinding, sawing, abrasive disc, plasma, or arc cutting to conform essentially with Figure 1 and shall be cleaned by wire brushing or grinding as necessary.  
B. When plasma or arc cutting is used, all oxides and scale shall be removed by machining or grinding away 1/16" of material.  
C. Prior to welding, the surface shall be free of oil, grease and excessive amounts of scale or rust.

Position:

- A. The welding may be done in the flat (1G, 1F), horizontal (2G, 2F), vertical (3G, 3F), overhead (4G, 4F), or multiple (5G, 6G) position.





WPS-9  
Rev. 11  
Page 2 of 4

B. The weld progression for positions 3G, 3F, 5G, and 6G shall be upward.

Preheat and Postheat Treatment:

- A. Preheat temperature - 50°F minimum.
- B. Interpass temperature - 350°F maximum.
- C. No postweld heat treatment required.

Electrical Characteristics:

- A. All welding shall be done with direct current, reversed polarity (base metal on negative side of line).

Joint Welding Procedure:

- A. The current and voltage shall be essentially as indicated in Table B.
- B. The welding sequence shall be essentially as shown in Figure 1 using stringer beads. The width of the bead shall not exceed 2-1/2 times the electrode diameter.
- C. Prior to welding the underside or second side of a groove, this side shall be backgrouged to clean metal by grinding, chipping, or arc gouging. Arc gouging shall be followed by grinding away 1/16" of material.
- D. Starts and stops which show excess reinforcement or excessive depressions shall be ground out prior to depositing next pass.

Cleaning:

- A. All slag or flux remaining on any bead of welding shall be removed before laying down the next successive bead of welding. Interpass cleaning shall be by wire brushing, grinding, or slag gun as necessary.

Defects:

- A. Any defects such as cracks, porosity, etc., which appear on the surface of any weld bead shall be removed by grinding, chipping, or arc gouging prior to the deposition of the next successive weld bead. Arc gouging shall be followed by grinding away 1/16" of material.
- B. Peening is prohibited.

Prepared by:

Reviewed by:

Jay Murphy  
Jay Murphy  
Quality Control Manager

Kamena P Singh  
Engineering



TABLE A

The following material - electrode combinations may be used unless specified otherwise on the shop drawings.

BASE MATERIAL	ELECTRODE
For Group P-8 materials of the following types:	
304 to 304	E308-15, E308-16
304L to 304L, 304	E308L-15, E308L-16
316 to 316, 304	E316-15, E316-16
316L to 316L, 316	E316L-15, E316L-16
317 to 317	E317-15, E317-16
317L to 317L, 317L	E317L-15, E317L-16
309 to 309	E309-15, E309-16

TABLE B

ELECTRODE SIZE	VOLTAGE RANGE	AMPERAGE RANGE	MIN. TRAVEL SPEED* (IPM)
3/32"	18-20	40-80	2-4
1/8"	20-22	80-120	4-7
5/32"	20-24	100-150	5-9
3/16"	20-24	130-190	6-11

\* As voltage and amperage are increased, the minimum travel speed shall be increased through the range indicated.



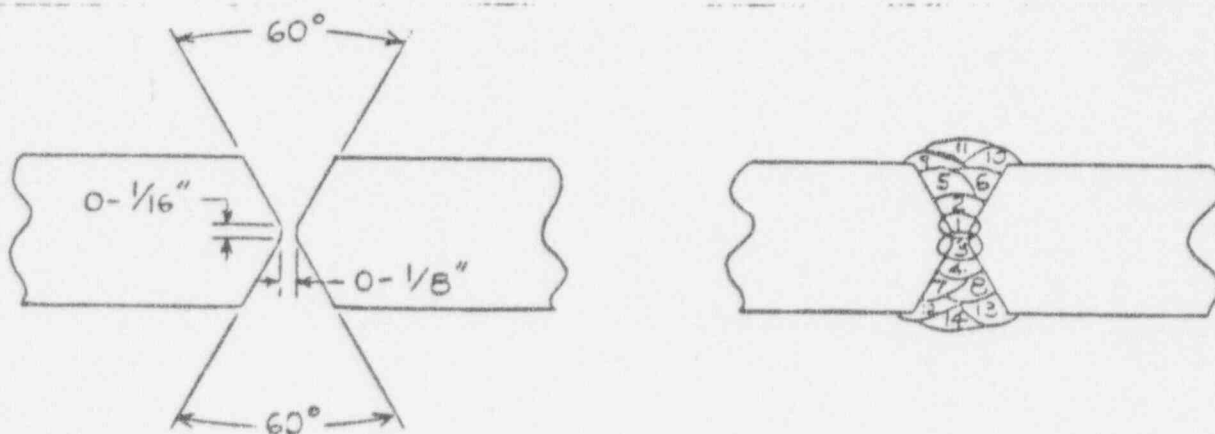
FIGURE 1

RECOMMENDED JOINT CONFIGURATIONS AND  
WELDING BEAD SEQUENCES\*

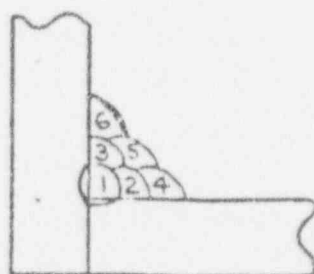
A. Material thicknesses of  $3/8"$  and less:



B. Material thicknesses greater than  $3/8"$ :



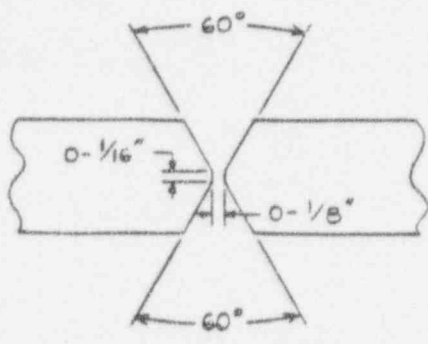
C. All thicknesses for any size fillet:



\*Other configurations acceptable upon Engineering approval.

QW-483 PROCEDURE QUALIFICATION RECORD (PQR)  
(Sec QW-201.2, Section IX, 1974 ASME Boiler and Pressure Vessel Code)

Company Name JOSEPH OAT CORPORATION  
Procedure Qualification Record No. PQR-9 Date 1/11/77  
WPS No. 9;  
Welding Process(es) SMAW Types Manual  
(Manual, Automatic Semi-Aut.)

<p><b>JOINTS (QW-402)</b></p> <div style="text-align: center;"><p>Groove Design Used</p></div>	<p><b>BASE METALS (QW-403)</b></p> <p>Material Spec. <u>SA-240</u></p> <p>Type or Grade <u>TP-304</u></p> <p>P No. <u>8</u> to P No. <u>8</u></p> <p>Thickness <u>3/4"</u></p> <p>Diameter <u>----</u></p> <p>Other <u>----</u></p>
<p><b>FILLER METALS (QW-404)</b></p> <p>Weld Metal Analysis A No. <u>8</u></p> <p>Size of Electrode <u>5/32"</u></p> <p>Filler Metal F No. <u>5</u></p> <p>SFA Specification <u>SFA 5.4</u></p> <p>AWS Classification <u>E-308-16</u></p> <p>Other <u>----</u></p>	<p><b>POSITION (QW-405)</b></p> <p>Position of Groove <u>Flat 1G</u></p> <p>Weld Progression <u>Forehand</u> (Uphill, Downhill)</p> <p>Other <u>----</u></p>
<p><b>POSTWELD HEAT TREATMENT (QW-407)</b></p> <p>Temperature <u>None</u></p> <p>Time <u>----</u></p> <p>Other <u>----</u></p>	<p><b>PREHEAT (QW-406)</b></p> <p>Preheat Temp. <u>50°F</u></p> <p>Interpass Temp. <u>350°F max.</u></p> <p>Other <u>----</u></p>
<p><b>ELECTRICAL CHARACTERISTICS (QW-409)</b></p> <p>Current <u>Direct</u></p> <p>Polarity <u>Reversed</u></p> <p>Amps. <u>130</u> Volts <u>22-24</u></p> <p>Travel Speed <u>10 ipm</u></p> <p>Other <u>----</u></p>	<p><b>GAS (QW-408)</b></p> <p>Type of Gas or Gases <u>None</u></p> <p>Composition of Gas Mixture <u>----</u></p> <p>Other <u>----</u></p>
	<p><b>TECHNIQUE (QW-410)</b></p> <p>String or Weave Bead <u>Stringer</u></p> <p>Oscillation <u>---</u></p> <p>Multipass or Single Pass <u>Multipass</u> (per side)</p> <p>Single or Multiple Electrodes <u>Single</u></p>

SPECIMEN NO.	WIDTH	THICKNESS	AREA	ULTIMATE TOTAL LOAD LB.	ULTIMATE UNIT STRESS PSI	CHARACTER OF FAILURE & LOCATION
9T1	1.569	0.731	1.147	97,250	84,790	Base Metal - Broke
9T2	1.569	0.724	1.136	96,000	84,510	Base Metal - Broke

TYPE AND FIGURE NO.	RESULT	TYPE AND FIGURE NO.	RESULT
QW-462.2(a)	Side- Satisfactory	QW-462.2(a)	Side-Satisfactory
QW-462.2(a)	Side- Satisfactory	QW-462.2(a)	Side-Satisfactory

[illegible]

FILLET WELD TEST (QW-180)

Result - Satisfactory \_\_\_\_\_ Penetration into Parent Metal \_\_\_\_\_  
 Yes, No Yes, No  
 Type and Character of Failure \_\_\_\_\_ Macro-Results \_\_\_\_\_  
 Welder's Name John F. Boyer Clock No. 72 Stamp No. \_\_\_\_\_  
 Tests conducted by: Pitts. Test Lab Laboratory Test No. 012676  
 per: R. D. Eavey

We certify that the statements in this record are correct and that the test welds were prepared, welded and tested in accordance with the requirements of Section IX of the ASME Code. \_\_\_\_\_

Signed Joseph Oat Corporation  
(Manufacturer)

Date 1/11/77

By Jan Murphy

(Detail of record of tests are illustrative only and may be modified to conform to the type and number of tests required by the Code.)

Joseph Oat Corporation Job No. J- 2267 210/4A  
 Customer VESTINGHOUSE P. O. # 546-AAZ-215350 RMP  
 Item No. \_\_\_\_\_ Dwg. No. \_\_\_\_\_ N.B. # \_\_\_\_\_  
 Code ASME III Class 2 Tube Side 3 Shell Side

INITIAL	DATE	INITIAL	DATE
Q.C. <u>JB</u>	<u>3/1/75</u>	A.I. <u>212</u>	<u>3/1/75</u>
ENG.		PPOD.	

Sheet 1 of 7  
 6-3-75 Revision 1

W=Denotes Westinghouse Hold Point.  
 AI=Denotes Code Hold Point.

NOTE: Initials Indicate acceptance.

STEP	DESCRIPTION	WELD PROC.		HOLD PT.	NDT PROC.		OAT INSP.		CUST. INSP.		AUTH INSP.	
		Number	Rev		Number	Rev	Sign	Date	Sign	Date	Sign	Date
I	MATERIAL RECEIPT											
	1. Shells											
	2. Heads											
	3. Nozzles											
	4. Tubes											
	5. Tube Sheets											
	6. Miscellaneous											
II	SHELL FABRICATION											
	1. Cut and roll shell plates to Dwg. Dimension (inspect).											
	2. Weld shell long seams inside background. (LPT)	22 35		AI	QC 100							
	3. Complete welding shell seams (LPT) (INSPECT)	22 35			QC 100							
	4. Fit-up shell sections.			AI								

Item No.

6-3-75 Revision I

[illegible]



Item No.

6-3-75 Revision 1

[illegible]



Item No.

Sheet 4 of 7

6-3-75 Revision 1

[illegible]

Item No.

6-3-75 Revision 1

[illegible]



Item No.

Revision 1 6-3-75

[illegible]

